

EXPERIMENTAL AND PHOTOGRAPHIC STUDY OF SURFACE
DISCHARGES ON DIFFERENT POLYMERIC MATERIALS

By

Y. Abed ✕

ABSTRACT:

A photographic investigation of the surface discharges on specimens of four polymeric materials is described. These materials are polystyrene, polyvinyl chloride, teflon and prespex. Tests are performed under A. C. voltage on square specimens each of side length 10 cm and thickness of 0.5 mm to 6mm in non-uniform field consisting of wire and plane electrodes. The wire electrode has diameters ranged from 0.3 mm to 6 mm. The inception voltage of the surface discharges is found to be dependent on both factors namely the wire diameter and material thickness. The relationship between this voltage and either of the two factors is proposed to be in the form of a straight line formula.

The surface discharges are recorded by a photographic camera using the four above-mentioned polymeric materials. The inception voltage is determined by means of an oscilloscope. Some selected close-up photographs are given here as example to demonstrate the nature of the surface discharges. The oscilloscope current traces of these discharges are also recorded by the camera and some of the reproduced photographs are also given for different wire diameters and material thickness.

INTRODUCTION:

The surface discharges formed on new organic insulating materials have been recently investigated because they are responsible for the electric breakdown of these materials. The new polymeric materials include polyethylene, polystyrene, polyvinyl chloride, prespex, teflon ... etc. They have wide applications in modern electrical equipments because they have excellent electrical properties.

In this paper, four types of polymeric insulating materials are investigated namely Polystyrene (P. S.), Polyvinyl Chloride (P. V. C.), Teflon (Polytetrafluoroethylene, P. T. F. E.) and Prespex (Polymethylmethacrylate, P. M. M. C.). The surface discharges formed under A. C. voltage on these materials are recorded using the close-up photography by a camera of type Zenit-E. They also are studied using an oscilloscope for varied

wire diameters and material thickness. A mathematical treatment is proposed to express the inception voltage in terms of these two factors namely the wire diameter and material thickness. A few number of the reproduced close-up photographs are given here to demonstrate the nature of the surface discharges, which are appeared on the oscilloscope and also recorded by the camera.

EXPERIMENTAL ARRANGEMENTS:

Two electrodes are arranged from a wire and a plane. The wire electrode is formed from solid copper conductors of 10 diameters ranged from 0.3 mm to 6 mm. The earthed plane electrode is an aluminium disc of 25 cm diameter and 3 mm thickness. The two electrodes and the specimen are installed in a dark box in the form of a cube of side length 30 cm.

A photographic camera of type Zenit-E is installed above the dark box. This camera has a Helios-44, f/2, 58 mm lens and a special arrangement to enable the close-up photography of the specimen under test. This arrangement consists of three pre-set extension tubes of 7 mm, 14 mm and 28 mm in length. The extension tubes give reproduction ratios down to 1 : 1. The camera is focussed on the specimen and therefore no part of the wire electrode is showed up in the photographs given in the present work. The photographs of the surface discharges are taken while the shutter is kept open during the voltage application. This photographic arrangement enables the observation and recording of the surface discharges during the experiments.

The specimens are square sheets with 10 cm side cut of 0.5 mm thick sheets which are readily available. Four types of polymeric materials are investigated here to study the formation of the surface discharges, which are mainly responsible of the breakdown of such modern insulating organic materials. The investigated materials are polystyrene, polyvinyl chloride, teflon and prespex. These materials have very high surface resistance and therefore they are mostly used to-day as insulating materials in high-voltage equipments.

The investigation of the surface discharges formed on the above-mentioned materials under A. C. high voltage obtained from a generating circuit supplied from the 220 V-supply. The applied voltage is measured by means of a resistive potential divider and electrostatic voltmeter. The formation of the surface discharges is assured by an oscilloscope connected across a 500-Ohm shielded resistance in series with the earthed plane electrode. The voltage applied to the specimen is gradually increased at a constant rate of 1 kV/sec till inception of the surface discharges is observed on the oscilloscope in the form of individual pulses superposed on the A. C. sine-wave. Each reading of the inception voltage represents the mean value of ten measurements using a new specimen for each voltage application to avoid any effect of the residual surface charges may be present on the specimen under test.

There is no guarantee with this approach, that the hopefully improved response is necessarily the best possible response of the system. The main goal of the present work is the introduction of a sensitivity technique suitable for adjusting the parameters of the feedforward controller in an optimum fashion. A practical system is used for illustration.

2. IMPROVED SENSITIVITY METHOD:

The improved sensitivity method⁽⁴⁾ requires only information about the output of the system. Perturbed output are obtained using a step signal at the controller reference input. Sensitivity functions are then expressed in terms of these perturbed outputs. These functions are used in predicting optimal settings for controller parameters. The equations which describe the model system with a controller in the feedback path, are:

$$y_i(s) = W_i(s) \cdot v(s) \text{ for } 1 \leq i \leq n \quad \dots\dots(1)$$

$$v(s) = K_r/s - \sum_{j=1}^n K_j \cdot y_j(s) \quad \dots\dots(2)$$

where y_i is the *i*th state variable,

W_i is the *i*th transfer function relation $y_i(s)$ to $v(s)$

v is the single input control,

K_r/s is the step disturbance of magnitude K_r ,

K_j is the *j*th feedback parameter, and

s is the laplace operator.

A quadratic system performance index is defined as:

$$J = \frac{1}{2} \int_0^{\infty} \left[\sum_{i=1}^n (y_{fi} - y_i) Q_i (y_{fi} - y_i) + (v_f - v) r (v_f - v) \right] dt \quad \dots\dots(3)$$

where y_f and v_f are final values of the system output and input, and Q_i and r are weighting factors. The sensitivity method computes the feedback parameters K so as to minimise the performance index J when the system is started from zero initial conditions ($y_0=0$) and permitted to settle to steady state conditions at which y is y_f .

Substitution of equation (2) into equation (1) gives:

$$y_i(s) = \frac{w_i(s) K_r/s}{1 + \sum_{j=1}^n K_j W_j(s)} \quad \dots\dots(4)$$

From our previous experience in designing feedback controller⁽⁴⁾ the step size K_r would be defined as an appropriate function of the feedback parameters. It takes the following form:

$$K_r = 1 + \sum_{j=1}^n K_j Y_{f,j} \quad \dots\dots(5)$$

This particular choice will make the feedback law equivalent to the one calculated using classical optimal control method, however with the advantage of on-site adjustment. The sensitivity of variable y_i with respect to parameter K_j is then expressed as follow:

$$S_{K_j}^{y_i} = \frac{\partial y_i}{\partial K_j} = \frac{\partial}{\partial K_j} \left(\frac{W_i(s)}{1 + \sum_{j=1}^n K_j W_j(s)} \right) \cdot K_r/s + \frac{1/s \cdot W_i(s)}{1 + \sum_{j=1}^n K_j W_j(s)} \cdot \frac{\partial K_r}{\partial K_j} \quad \dots\dots(6)$$

For computational purposes this equation is reformulated in sampled data form as:

$$S_{k_j}^{y_i}(\gamma \cdot \Delta t) = \frac{1}{K_r} \left[\sum_{\beta=1}^{\gamma} - \frac{y_i(\beta \cdot \Delta t) - y_i(\beta-1) \cdot \Delta t}{t} \right. \\ \left. y_j(\gamma, \Delta t - \beta \cdot \Delta t) \right] + \frac{1}{K_r} \cdot y_{f_j} \cdot y_i(\gamma \cdot \Delta t) \dots (7)$$

Where:

- γ = number of samples
- Δt = sampling interval
- $y_i(0) = 0$ for $1 \leq i \leq n$.

It should be noted that the accuracy of the sensitivity function, equation (7), depends upon the value taken for the time interval Δt . The smaller this value, the higher is the accuracy. On the other hand, the choice of a very small time interval makes the use of this algorithm costly in computer time. A value of 0.02 second for Δt is found suitable.

Hjk it has been shown⁽⁴⁾ that the sensitivity functions, given by equation (7), can be used to calculate the feedback parameters K_j for all j .

3. SENSITIVITY FUNCTION FOR FEEDFORWARD-PATH CONTROLLER:

The model system with a controller in the forward path is shown in Fig.(1). However, this schematic diagram differs from the conventional feedforward controller in that, its parameters is adjusted on-site based on sensitivity measure equation (7). Moreover the design procedure does not require prior knowledge of the parametric structure of the controlled system. This point offers great advantages when we are dealing with a large scale system like a power plant.

Element of Fig.(1) are:

$C(s, \alpha_j)$ $j = 1, m$ is a controller with m adjustable parameters.

$W(s)$ is unidentified system which is being controlled.

$y_i(s)$ $i = 1, n$ is the resultant change in the i th output.

$G_i(s)$ is the transfer function relation $T(s)$ to $y_i(s)$.

$V_r(s)$ is a step disturbance to the controller reference.

K_r is a scaling factor.

The following relations can be easily obtained from Figure (1);

$$E(s) = V_r(s) - y_i(s) \dots\dots(8)$$

$$y_i(s) = E(s) C(s, \alpha_j) W(s) G_i(s) \dots\dots(9)$$

$$V_r(s) = K_r/s \dots\dots(10)$$

Using equations (8, 9) and (10) we obtain;

$$y_i(s) = \frac{W(s) C(s, \alpha_j) G_i(s)}{1 + C(s, \alpha_j) W(s) G_i(s)} K_r/s \dots\dots(11)$$

The sensitivity function of the state variable y_i with respect to the adjustable parameter α_j is defined as⁽⁴⁾

$$S_j^{y_i} = K_r/s \frac{\partial}{\partial \alpha_j} \left(\frac{W(s) C(s, \alpha_j) G_i(s)}{1 + C(s, \alpha_j) W(s) G_i(s)} \right) + \frac{W(s) C(s, \alpha_j) G_i(s)}{1 + C(s, \alpha_j) W(s) G_i(s)} \frac{\partial K_r}{\partial \alpha_j} \dots\dots(12)$$

Since the controller function is to improve the dynamic response of the system due to unpredictable changing conditions a proper form would be:

III. COMPUTED CORONA VOLTAGE:

1. Peek's Formula:

The visual corona voltage between two parallel conductors can be calculated by Peek's empirical equation. This equation is well known for electrical engineers and has the following form:

$$V_v = 30 m\delta r \left(1 + \frac{0.301}{\sqrt{\delta r}}\right) \ln \frac{D}{r} \quad \dots(1)$$

where,

V_v = visual corona voltage to neutral, kV (peak)

m = surface condition factor

= 0.9 for solid conductors

= 0.8 for stranded conductors

δ = air density factor = 1 at N.T.P.

r = conductor radius in cm

D = gap distance in cm.

2. Computed Visual Corona Voltages:

As a comparison, Peek's empirical equation is applied to calculate the visual corona voltage for the mentioned conductor diameters and gap distances. The computed values obtained on applying Peek's equation are also illustrated in Fig.(1) by the dotted lines. The percentage error obtained on applying Peek's equation does not exceed $\pm 8\%$ of the experimental values for the mentioned conductors and gap distances. This error is resulted from factors related to both the measuring technique and Peek's formula. In the former, visual corona is checked visually and by means of an oscilloscope while in the second only visually. Therefore the experimental values of corona voltage may be considered as more exact values than those given by Peek's formula.

IV. PROPOSED MODIFICATION:

The effect of enviromental conditions are not considered in Peek's equation to compute the voltage of visual corona formed between parallel wires. Therefore this formula gives higher corona voltages than the actual values. As a proposed modification for Peek's equation, the enviromental conditions are considered to give exact values of visual corona voltage between parallel wires. The proposed modification can be applied in two cases namely pure moisture and wet pollution as follows.

1. Pure Moisture:

In this case the modified equation gives the voltage of visual corona as a function of the relative humidity of air in exponential form as follows:

$$V_v = 30 m \sqrt{r} w^{-a} \left(1 + \frac{0.301}{\sqrt{\delta r}} \right) \ln \frac{D}{r} \dots(2)$$

where,

w = the percentage relative humidity

a = constant depending on the power system.

The value of this constant is found to be a = 0.18 under the experimental conditions and for the prementioned conductors.

As a comparison, the proposed modification is checked by computing the corona voltage at different relative humidities. Figure (3) illustrates these values (dotted curves) compared with those obtained experimentally (solid curves). The percentage error is calculated for different values of relative humidity for the given conductor diameters and found to be of comparatively low values. The maximum percentage error attained on applying Eqn. (2) is

not higher than 8%, which can be considered as good accepted value.

2. Wet Pollution:

Here, the proposed modification can be also used to estimate the voltage of visual corona in air between the parallel conductors. This voltage can be expressed under wet pollution as:

$$V_v = 30 m \delta r w^{-b} \left(1 + \frac{0.301}{\sqrt{\delta r}} \right) \ln \frac{D}{r} \quad \dots(3)$$

where,

b = constant depending on the power system and type of pollution.

The constant (b) is found to be b = 0.22 under the experimental conditions discussed before.

Figure (3) illustrates both the experimental and computed values of the voltage of the visual corona formed in humid polluted air between parallel wires of different diameters and at 15 cm spacing from each other. Here, also the thicker conductor gives higher voltages of visual corona under the same relative humidity. As a numerical example at 50% relative humidity under artificial polluted conditions, the visual corona voltage is 25 kV for gap 15 cm long and conductor diameter 4.5 mm while the corresponding value is only 10 kV for conductor diameter 0.3 mm under the same conditions. The percentage error attained on applying the proposed modification under wet polluted conditions is comparatively higher than under dry conditions. The maximum error in this case does not exceed $\pm 10\%$ of the experimental values of the visual corona voltage.

V. CONCLUSIONS:

The visual corona voltage of atmospheric air is strongly reduced by the environmental moisture and pollution. This reduction effect is taken into account and a proposed modification for Peek's equation is given. The visual corona voltage can be calculated in terms of the percentage relative humidity of air between parallel wires. Under polluted humid conditions the reduction effect will be higher. The proposed modification gives values of visual corona voltage close to those obtained experimentally in high voltage laboratory. The maximum percentage error attained on applying this modification does not exceed $\pm 10\%$ of the corresponding experimental values.

REFERENCES:

1. ALAN H. COOKSON, ROY E. WOTTON, "A.C. Corona and Break-down Characteristics for Rod Gaps in Compressed Hydrogen, SF₆ and Hydrogen-SF₆ Mixture", IEEE Trans., Vol. PAS-97, 1978, pp 415.
2. HAHN G., ZACKE P., FISHER A. AND BOECKER H., "Humidity Influence on Switching Impulse Breakdown of a 50 cm Rod-Plane Gap", IEEE Trans., Vol. PAS-95, 1976, pp. 1145-1152.
3. HASSAN S. A., ABED Y. AND EL-ZEFTAWY, "Factors affecting Corona Characteristics of thin Wires", Mansoura Bulletin, Vol. 5, 1980, pp. 40-57.
4. IEEE COMMITTEE REPORT, "Sparkover Characteristics of High-Voltage Protective Gaps", IEEE Trans., Vol. PAS-93, 1974, pp. 196.
5. LOEB L. B., "Electrical Coronas", 1965, University of California Press, USA.
6. TRINH N. GIAO AND JAN B. JORDAN, "Modes of Corona Discharges in Air", IEEE Trans., Vol. PAS-87, 1968, pp. 1207-1215.

E.30. Y.Abed, Tantawy & El-Maghraby

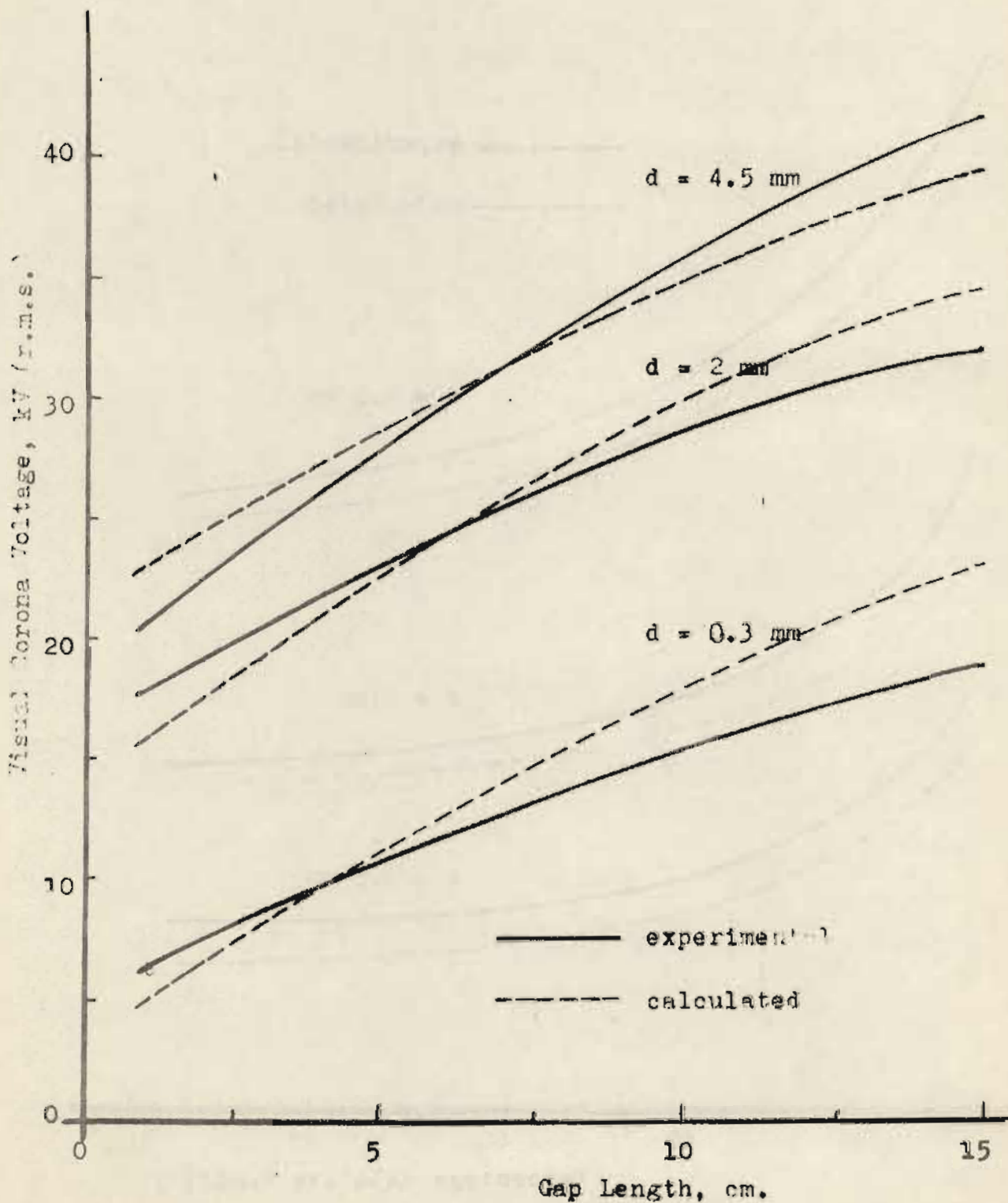


FIG. 1: The visual corona voltage of air versus the distance between parallel wires having different conductor diameters.

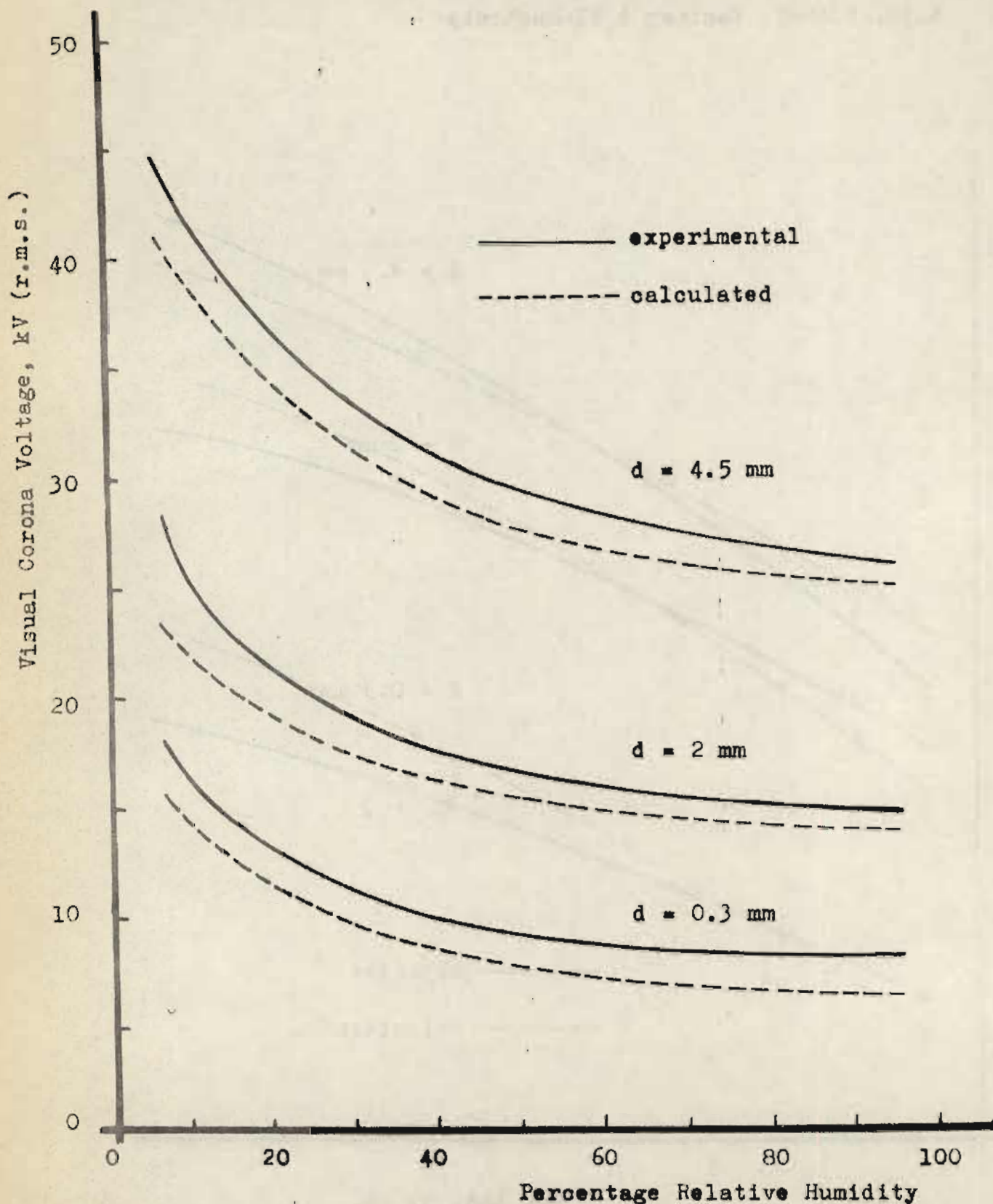


Fig. 2: The effect of moisture on visual corona voltage of air gap 15 cm long between parallel wires of different diameters.

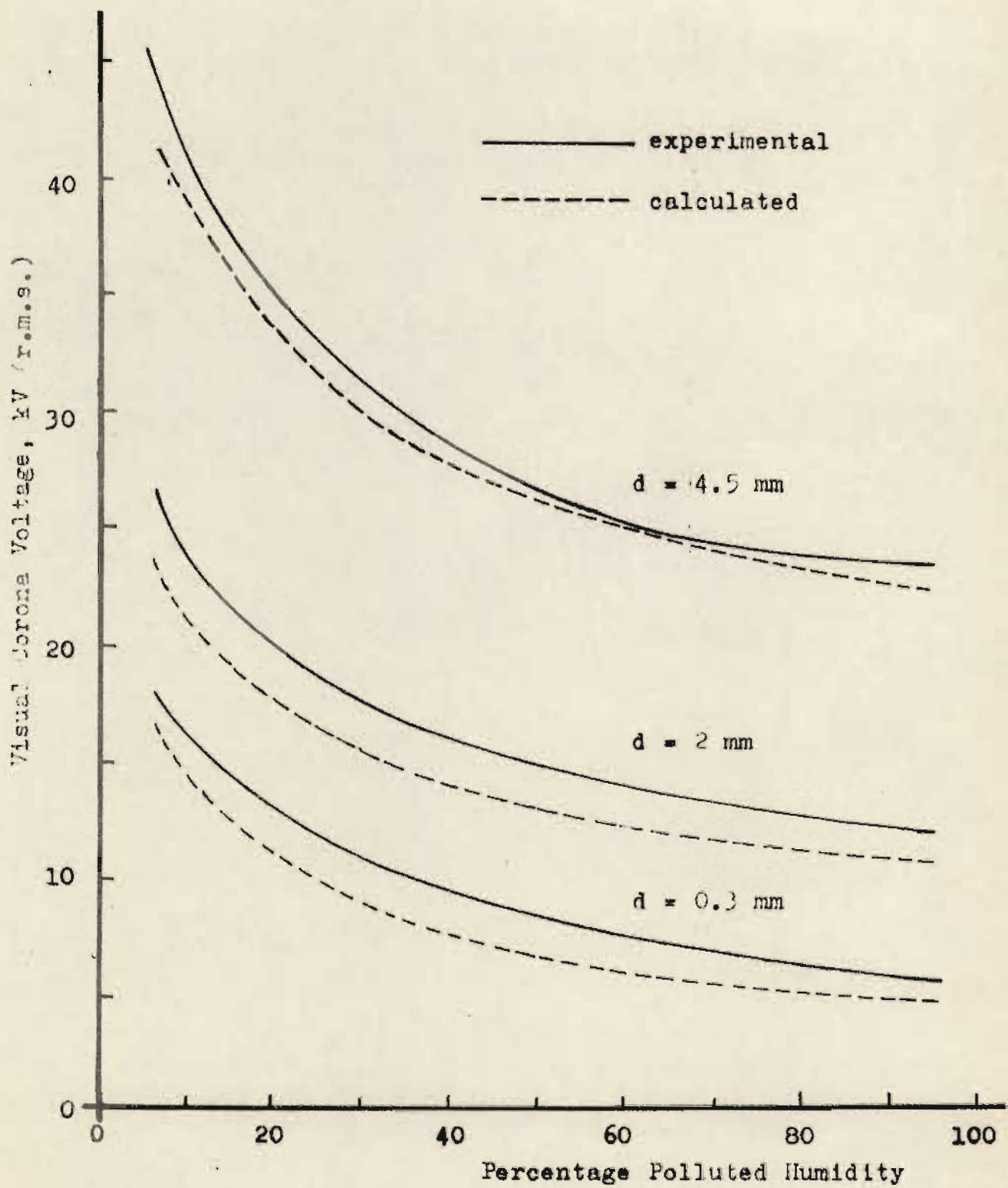


Fig. 3: The effect of moistened pollution on visual corona voltage of air between parallel wires of different diameters at 15 cm spacing from each other.